A Proofs

Theorem 1. *Let the parameters of InDI [9] in Table 1 be* $t := \frac{\gamma_t^2}{\gamma_t^2+\bar{\gamma}_t^2}$, $\epsilon_t^2 := \frac{\bar{\gamma}_t^2}{\gamma_t^2}(\gamma_t^2 + \bar{\gamma}_t^2)$. *Then, InDI and* I^2*SB are equivalent.*

Proof. In order to proceed with the proof, we first remind the notations from Table 1:

$$\gamma_t^2 := \int_0^t \beta_\tau \, d\tau, \quad \bar{\gamma}_t^2 := \int_t^1 \beta_\tau \, d\tau. \tag{17}$$

By definition, we note that $\gamma_t^2 + \bar{\gamma}_t^2 = \int_0^1 \beta_\tau \, d\tau$ is constant for any choice of $t \in [0, 1]$. To proceed with the proof, we have for $\alpha_{s|t}^2$,

$$s/t = \frac{\gamma_s^2}{\gamma_s^2 + \bar{\gamma}_s^2} / \frac{\gamma_t^2}{\gamma_t^2 + \bar{\gamma}_t^2} = \frac{\gamma_s^2}{\gamma_t^2}. \tag{18}$$

Considering $\sigma_{s|t}^2$,

$$s^2(\epsilon_s^2 - \epsilon_t^2) = \frac{\gamma_s^4}{(\gamma_s^2 + \bar{\gamma}_s^2)^2} \left(\frac{\bar{\gamma}_s^2}{\gamma_s^2}(\gamma_s^2 + \bar{\gamma}_s^2) - \frac{\bar{\gamma}_t^2}{\gamma_t^2}(\gamma_t^2 + \bar{\gamma}_t^2) \right) \tag{19}$$

$$= \frac{\gamma_s^4}{\gamma_s^2 + \bar{\gamma}_s^2} \left(\frac{\bar{\gamma}_s^2}{\gamma_s^2} - \frac{\bar{\gamma}_t^2}{\gamma_t^2} \right) \tag{20}$$

$$= \frac{\gamma_s^2}{\gamma_s^2 + \bar{\gamma}_s^2} \left(\frac{\bar{\gamma}_s^2 \gamma_t^2 - \bar{\gamma}_t^2 \gamma_s^2}{\gamma_t^2} \right) \tag{21}$$

$$\overset{\text{(a)}}{=} \frac{\gamma_s^2}{\gamma_s^2 + \bar{\gamma}_s^2} \frac{d_s^2(\gamma_t^2 + \bar{\gamma}_t^2)}{\gamma_t^2} \tag{22}$$

$$= \frac{\gamma_s^2}{\gamma_t^2} d_s^2 \tag{23}$$

$$= \frac{\gamma_s^2}{\gamma_t^2}(\gamma_t^2 - \gamma_s^2), \tag{24}$$

where in (a), we defined $d_s^2 := \int_s^t \beta_\tau, d\tau$ such that $\gamma_s^2 + d_s^2 = \gamma_t^2$ is satisfied. □

Theorem 2. *The total variance condition* (12) *is satisfied for both* I^2*SB and InDI.*

Proof. Here, we further show that the condition is satisfied for I^2SB for completeness.

$$\sigma_s^2 - (\alpha_{s|t}^2)^2 \sigma_t^2 = \frac{\gamma_s^2 \bar{\gamma}_s^2}{\gamma_s^2 + \bar{\gamma}_s^2} - \frac{\gamma_s^4}{\gamma_t^4} \frac{\gamma_t^2 \bar{\gamma}_t^2}{\gamma_t^2 + \bar{\gamma}_t^2} \tag{25}$$

$$= \frac{\gamma_s^2}{\gamma_s^2 + \bar{\gamma}_s^2} \left(\bar{\gamma}_s^2 - \frac{\gamma_s^2}{\gamma_t^2} \bar{\gamma}_t^2 \right) \tag{26}$$

$$= \frac{\gamma_s^2}{\gamma_t^2} \frac{\bar{\gamma}_s^2 \gamma_t^2 - \gamma_s^2 \bar{\gamma}_t^2}{\gamma_s^2 + \bar{\gamma}_s^2} \tag{27}$$

$$= \frac{\gamma_s^2}{\gamma_t^2} \frac{(\bar{\gamma}_t^2 + d_s^2)\gamma_t^2 - \gamma_s^2(\gamma_t^2 - d_s^2)}{\gamma_s^2 + \bar{\gamma}_s^2} \tag{28}$$

$$= \frac{\gamma_s^2}{\gamma_t^2} \frac{d_s^2(\gamma_t^2 + \bar{\gamma}_t^2)}{\gamma_s^2 + \bar{\gamma}_s^2} \tag{29}$$

$$= \frac{\gamma_s^2(\gamma_t^2 - \gamma_s^2)}{\gamma_t^2} = \sigma_{s|t}^2, \tag{30}$$

where we use $\gamma_s^2 + d_s^2 = \gamma_t^2$ for the last equality. □

B Details on Table 1

I²SB $\beta_{\min} = 0.0001$, $\beta_{\max} = 0.02$. The same β_t schedule is used regardless of being implemented as deterministic or not. For the former, $\sigma_t = \sigma^2_{s|t} = 0$.

InDI The speed of the base degradation process is parametrized with constant time-speed t. For deterministic methods, $\epsilon_t = 0$ and hence $\sigma_t = \sigma^2_{s|t} = 0$. For stochastic methods, $\epsilon_t = 0.01$ such that $\sigma^2_{s|t} = 0$.

IR-SDE (PF-ODE) As mentioned in the main text, IR-SDE can also be considered a type of DDB as it obeys the marginal distribution that is characterized by (8), but with a different sampling method. Specifically, we can set $\alpha_t = 1 - e^{-\bar{\theta}_t}$, $\sigma_t^2 = \lambda^2(1 - e^{-2\bar{\theta}_t})$, with $\delta = 0.008$. λ^2 is the stationary variance of the OU-process, which is set to the noise variance of the degraded image. For all non-noisy inverse problems that we mostly consider in this work, λ^2 is still set to $10/255$.

C Experimental Details

C.1 Implementation Details

Models All the models that are used throughout the work are based on pre-trained models from I²SB[5]. All the models are fine-tuned from the ADM [11] ImageNet 256×256 model, hence share the same architecture as well as the specific model hyper-parameter settings.

Inverse problem setting All the forward operators $\boldsymbol{A}$ are used in the same manner as in [26], which are adopted from DDRM [21].

Step size, gradient For both Algorithms 1,2, we use constant step size, but scaled to match the signal ratio of the intermediate reconstructions $\hat{\boldsymbol{x}}_{0|i}$: $\rho_i = (1 - \alpha^2_{i|i+1})c$, where c is some constant. For SR and deblurring tasks, we take $c = 1.0$. For JPEG restoration, we take $c = 0.5$.

When implementing the gradient computation for CDDB, we do not explicitly compute $\boldsymbol{A}^\top$, but rely on automatic differentiation for simplicity. This lets us unify the implementations of Algorithm 1,2 in a similar manner.

Compute All experiments were run using a single RTX 3090 GPU. On average, I²SB and CDDB with 1000 NFE take about 82 seconds ($\sim$ 0.08 sec. / iter). CDDB-deep takes about 193 seconds ($\sim$ 0.19 sec. / iter).

Code Availability Code is available at `https://github.com/HJ-harry/CDDB`

C.2 Comparison Methods

I²SB We follow the default setting advised in [26] and set the default sampling schedule to be the quadratic schedule [35] with 1000 NFE. As we leverage the pre-trained checkpoints provided, deblurring and inpainting models are set to OT-ODE with no additive Gaussian noise during the sampling process.

DPS, ΠGDM Pre-trained ADM models that were used in the original work [5, 36] are used. For DPS, we use the constant step size of 1.0 with 1000 NFE. For ΠGDM , we use the constant step size of 1.0 with 100 NFE. We initially experimented with higher NFE for ΠGDM but did not find a boost in performance.

DDRM We use 20 NFE DDIM sampling with $\eta = 0.85$, $\eta_b = 1.0$ as advised.

DDNM We use 100 NFE sampling with $\eta = 0.85$ as advised. We do not use time travel for all experiments.

[5]https://github.com/NVlabs/I2SB

	CDDB								CDDB-deep							
$c =$	0.0	0.25	0.5	0.75	1.0	1.5	2.0	3.0	0.0	0.25	0.5	0.75	1.0	1.5	2.0	3.0
PSNR (↑)	25.07	26.14	26.28	**26.31**	**26.31**	26.30	26.24	25.70	25.07	26.21	26.42	26.51	26.56	**26.59**	26.57	26.06
SSIM (↑)	0.692	0.744	0.752	**0.753**	**0.753**	0.751	0.747	0.729	0.692	0.745	0.756	0.760	0.761	**0.762**	0.760	0.747
LPIPS (↓)	0.271	0.218	0.206	0.203	**0.201**	0.202	0.207	0.244	0.271	0.226	0.214	0.209	0.205	**0.202**	**0.202**	0.227
FID (↓)	37.78	32.81	30.76	29.89	29.33	**28.99**	29.85	37.22	37.78	35.07	33.17	32.25	**29.29**	29.97	29.71	34.22

Table 4: Step size ablation on the step size for CDDB $c := \rho_i/(1-\alpha^2_{i|i+1})$ using 100 test images on SR×4-bicubic task, NFE=100. I[2]SB [26], Chosen step size.

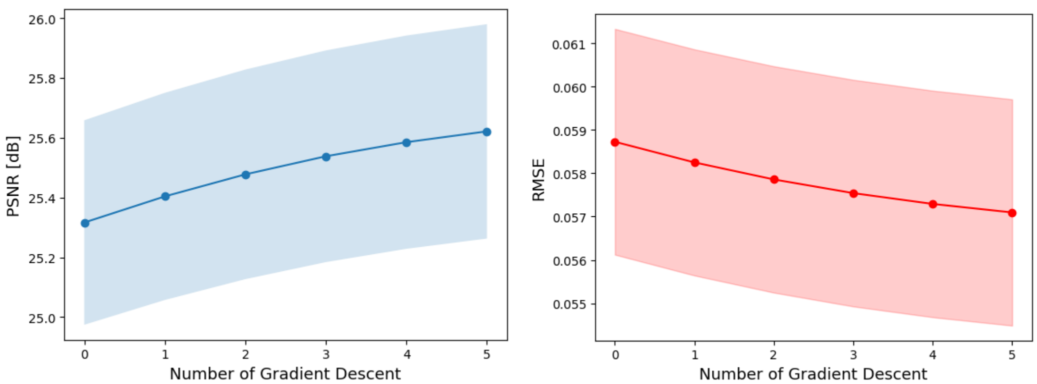

(a) # GD steps vs. PSNR (↑)

(b) # GD steps vs. RMSE (↓)

Figure 6: Effect of gradient descent (GD) steps in CDDB applied to intermediate samples $\hat{\boldsymbol{x}}_{0|i}$. Mean $\pm$ 0.1 std indicated as colored region.

DDS We use 100 NFE sampling with $\eta = 0.85$ since we did not observe additional performance gain with larger NFE.

PnP-ADMM, ADMM-TV Following [5], we use the implementation provided in the `scico` library [2]. For PnP-ADMM, we use $\rho = 0.2$, `maxiter`$= 12$ with the DnCNN [42] denoiser. For ADMM-TV, we use as the regularization term $\lambda\|\boldsymbol{D}\boldsymbol{x}_0\|_{2,1}$ with $(\lambda, \rho) = (2.7e-2, 1.4e-1)$ for deblurring and $(\lambda, \rho) = (2.7e-2, 1.0e-2)$ for SR.

C.3 Evaluation

Out of the default 10k evaluation images from 256×256 ImageNet [10] used in [26], we use 1k images by interleaved sampling: i.e. Images of index 0, 10, 20, . . . are used. When computing the FID score, we use the `pytorch-fid` package and compare the distribution of the ground truth images vs. the reconstructed images, rather than comparing against the training data, following the setting of [5].

D Ablation Studies

D.1 Step size

In Table 4, we summarize the effect of the choice of step size when implementing CDDB/CDDB-deep. Note that for *all* choice of step sizes, the quantitative metrics are superior to the I[2]SB counterpart, which states that CDDB stably improves the performance. We observe that for both methods, $c = 1.0$ strikes a good balance between the distortion and the perception metrics. For CDDB-deep, taking a slightly larger step size (e.g. $c = 1.5$) improves performance for certain problems, but we keep $c = 1.0$ for unity.

D.2 Effect of gradients during sampling

In Fig. 6, we investigate the effect of the CDDB gradient steps when applied to $\hat{\boldsymbol{x}}_{0|i}$ (i.e. intermediate denoised estimate) with $i = N//2^6$, 10 NFE for 300 test samples on SR×4-bicubic task. Note that we can apply multiple GD steps to the intermediate denoised sample $\hat{\boldsymbol{x}}_{0|i}$, which is indicated in the x-axis of the figures. Even when we apply multiple GD steps, we observe that the metrics constantly get better, establishing the stability of the proposed method.

[6] python notation